AMERICAN ACADEMY™ OF OPHTHALMOLOGY

Microstructure of Peripapillary Atrophy and Subsequent Visual Field Progression in Treated Primary Open-Angle Glaucoma

Hiroshi Yamada, MD, Tadamichi Akagi, MD, PhD, Hideo Nakanishi, MD, PhD, Hanako O. Ikeda, MD, PhD, Yugo Kimura, MD, PhD, Kenji Suda, MD, Tomoko Hasegawa, MD, Munemitsu Yoshikawa, MD, Yuto Iida, MD, Nagahisa Yoshimura, MD, PhD

Purpose: To investigate the relationship between the microstructure of β-zone peripapillary atrophy (PPA) and the subsequent visual field (VF) progression in eyes with primary open-angle glaucoma (POAG), including highly myopic eyes.

Design: Retrospective cohort study.

Participants: A total of 129 patients with POAG who had been followed up for a minimum of 2 years and had undergone at least 5 reliable standard automated perimetry tests after spectral-domain (SD) optical coherence tomography (OCT) examination.

Methods: β-Zone PPA was evaluated from 3 SD OCT scans centered on the optic disc. Upper and lower scans were defined as scans at 30° above and below the horizontal scan, respectively. From 3 scans of each eye, β-zone PPA was classified as PPA_{+BM} or PPA_{-BM} on the basis of the presence or absence of Bruch's membrane (BM), respectively. Eyes were classified into 3 groups according to the horizontal scan images: group A (only PPA_{+BM}), group B (both PPA_{+BM} and PPA_{-BM}), and group C (only PPA_{-BM}). Factors associated with the subsequent mean deviation (MD) slope after OCT examination were analyzed, and the hemifield total deviation (TD) slope was assessed in eyes with unilateral hemifield VF defects in the corresponding direction.

Main Outcome Measures: Subsequent MD slope after OCT examination.

Results: The VF progression in group A was faster than in group C ($P = 0.004$). A larger PPA_{+BM} width was associated with a faster MD slope in all eyes ($P < 0.001$) and highly myopic eyes ($P < 0.001$) and with a faster TD slope in eyes with superior or inferior hemifield VF defects in the corresponding direction ($P = 0.002$ and $P = 0.035$, respectively). A larger PPA_{-BM} was correlated with a slower MD slope in all eyes ($P = 0.030$ and $P = 0.034$) but not in highly myopic eyes.

Conclusions: There were significant differences in VF progression according to the microstructure of the β-zone PPA in eyes with POAG. The PPA_{+BM} width may be an important risk factor for VF progression in POAG, including high myopia, and the PPA_{-BM} width may have a protective effect for VF progression in this subtype of POAG. *Ophthalmology 2016;123:542-551 © 2016 by the American Academy of Ophthalmology.*

Supplemental material is available at www.aaojournal.org.

Peripapillary atrophy (PPA) can be subdivided into α-zone and β-zone subtypes.[1] The α-zone PPA is characterized by irregular hypopigmentation and hyperpigmentation of the retinal pigment epithelium, located in the periphery of the PPA. The β-zone PPA is characterized by atrophy of the retinal pigment epithelium and choriocapillaries, visible sclera, and large choroidal vessels, located between the optic disc and the α-zone.[1,2] Several previous studies have shown that β-zone PPA is associated with the incidence and progression of glaucoma.[1–8] Peripapillary atrophy also has been commonly reported in highly myopic eyes;[9–11] however, the relationship between PPAs in glaucoma and myopia is not fully understood.

Jonas et al[12] histologically subdivided classic β-zone PPA into newly defined β-zone PPA existing with Bruch's membrane (BM) (PPA_{+BM}) and newly defined γ-zone PPA containing no overlying BM (PPA_{-BM}). This showed that PPA_{+BM} is associated with glaucoma but not with myopia, whereas PPA_{-BM} is unrelated to glaucoma but related to myopia. However, the authors of this histologic study reported several potential limitations, such as measurement deviations in tissue preparation, sampling bias, and insufficient clinical data.

Recent studies have demonstrated that BM opening is easily detectable using spectral-domain optical coherence tomography (SD OCT).[13–17] The PPA_{+BM}, but not

http://dx.doi.org/10.1016/j.ophtha.2015.10.061
ISSN 0161-6420/15

PPA_{-BM}, was found to be associated with the presence of glaucoma using SD OCT;[15] this was consistent with the findings of the previous histologic study.[12] Kim et al[13] demonstrated that glaucomatous eyes exhibiting only PPA_{+BM} demonstrate a faster rate of retinal nerve fiber layer thinning than eyes with PPA_{-BM} only. This suggests that the presence of PPA_{+BM} may be a risk factor for progressive glaucomatous visual field (VF) defects. However, it has not been validated whether the progression of glaucomatous VF defects varies according to different microstructures of the β-zone PPA. Furthermore, it is unknown whether PPA_{+BM} in highly myopic eyes is associated with the presence or progression of glaucoma, as reported in nonhighly myopic eyes.

In the current study, we investigated the relationship between the microstructure of β-zone PPA and the subsequent VF progression to determine the potential of β-zone PPA microstructure as a predictive factor for future glaucoma progression in glaucomatous eyes, including highly myopic eyes.

Methods

Subjects

Subjects examined by radial scans of the optic disc using an SD OCT system (Spectralis HRA+OCT, Heidelberg Engineering, Heidelberg, Germany) at the glaucoma service in Kyoto University Hospital between November 5, 2007, and June 15, 2012, were candidates for this retrospective cohort study. The study and data collection adhered to the tenets of the Declaration of Helsinki and were approved by the Institutional Review Board and Ethics Committee of Kyoto University Graduate School of Medicine. All participants consented to the ophthalmic examinations before they were performed.

All subjects in the database had already undergone a comprehensive ophthalmic examination, including best-corrected visual acuity (BCVA) measurement (5 m Landolt chart), refraction, keratometry, slit-lamp examination, axial length measurement (IOLMaster 500, Carl Zeiss Meditec, Dublin, CA), central corneal thickness (SP-3000, Tomay, Tokyo, Japan), optic disc size on clinical examination (Heidelberg Retina Tomography 2, Heidelberg Engineering), Goldmann applanation tonometry, gonioscopy, indirect ophthalmoscopy, dilated slit-lamp optic nerve head examination, fundus photography, stereo disc photography (3-Dx simultaneous stereo disc camera, Nidek, Gamagori, Japan), red-free fundus photography (Heidelberg Retina Angiography 2, Heidelberg Engineering), standard automated perimetry (SAP) (Humphrey Visual Field Analyzer, Carl Zeiss Meditec) with the 24-2 Swedish Interactive Threshold Algorithm standard program, and SD OCT. The baseline intraocular pressure (IOP) was defined as the average of the 2 measurements obtained on the first day and at the following SD OCT examination date. Mean IOP measurements were obtained by averaging all IOP measurements during follow-up, and IOP fluctuation was determined using the standard deviation of these values.

We only included subjects with primary open-angle glaucoma (POAG) who had been followed up for at least 2 years and had undergone at least 5 reliable SAP tests after the SD OCT examination date. Primary open-angle glaucoma was defined as the presence of a normal anterior chamber on slit-lamp, normal open angle on gonioscopy, glaucomatous appearance of the optic disc, or retinal nerve fiber layer defects that corresponded with typical reproducible VF defects on SAP, as confirmed by 2 reliable consecutive tests. We excluded those with opaque media, diabetic retinopathy, or other ophthalmic diseases that could cause VF defects or fundus abnormalities, history of eye trauma or intraocular surgery other than cataract and glaucoma surgery, history of systemic or neurologic diseases that can affect the VF, and those with a BCVA <20/40. If subjects underwent cataract or glaucoma surgery during follow-up, we included only those who met the inclusion criterion before surgery. When both eyes of a subject were eligible, 1 eye was randomly selected for the study. In this study, high myopia was defined by an axial length exceeding 26 mm.

Visual Field Assessment

The criteria of Anderson and Patella[18] was used to define glaucomatous VF results on SAP: glaucoma hemifield test outside normal limits, pattern standard deviation probability <5%, or a cluster of 3 or more adjacent nonedge points in typical glaucomatous locations that did not cross the horizontal meridian (all of which were depressed on the pattern deviation plot at a $P < 5\%$; 1 of which was depressed at a $P < 1\%$ level on at least 2 consecutive plots). Visual field results were considered reliable on the basis of a fixation loss ≤15%, a false-positive ≤15%, and a false-negative ≤15%.

Glaucomatous unilateral hemifield VF defects were defined as VF defects according to Anderson and Patella's criteria in the superior or inferior hemifield only.

Spectral-Domain Optical Coherence Tomography Imaging of β-Zone Peripapillary Atrophy Area

The Spectralis HRA+OCT system was used to scan the optic disc including the PPA before the sequence of SAP tests. Tomographic images of the optic disc were obtained with infrared (IR) fundus images acquired simultaneously using a confocal scanning laser ophthalmoscope. Our disc scan protocol comprised 6 raster scan lines with a scan length of 6 mm centered on the optic disc (not based on BM opening), and the B-scan image on each scan line was obtained by averaging 50 scans. This study obtained 3 B-scans: horizontal scans and upper and lower scans that were defined as scans 30° above and below the horizontal scan, respectively (Fig 1).

β-Zone Peripapillary Atrophy Area Measurements

The structure of the temporal β-zone PPA and optic disc was analyzed with the intrinsic viewer (Heidelberg Eye Explorer software version 1.7.0.0; Heidelberg Engineering). This viewer automatically synchronizes the vertical lines of each B-scan and IR image. The distance between 2 arbitrary points, measured with intrinsic calipers, was used to correct for the effect of corneal curvature. The temporal β-zone PPA margin, BM opening, and disc margin were defined using IR and B-scan images magnified to 200% by the first examiner (H.Y.), in a masked fashion. The temporal disc margin and β-zone PPA margin was defined as the border between low and high reflectivity on IR images. The BM opening was identified on optical coherence tomography (OCT) B-scans as the termination of highly reflective continuous lines (Fig 1). Eyes were excluded when these points could not be clearly identified.

On the basis of the location of BM opening within the β-zone PPA area, β-zone PPA was subdivided into PPA_{+BM}, the zone from β-zone PPA margin to BM opening, and PPA_{-BM}, the zone from BM opening to the disc margin. The widths of β-zone PPA,

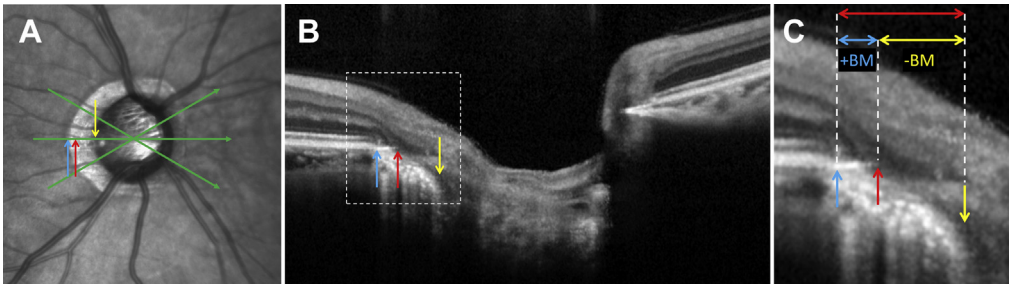

Figure 1. Microstructure of β-zone peripapillary atrophy (PPA). **A,** Infrared (IR) fundus image of the optic disc. The 3 *green arrowed lines* indicate the scanned locations centered on the optic disc. The 3 B-scans comprise horizontal and upper and lower scans, defined as scans 30° above and below the horizontal scan, respectively. **B,** Spectral-domain optical coherence tomography (SD OCT) B-scan image of the location indicated by *horizontal green arrowed line* in **A**. **C,** Magnified image of the rectangular area indicated by *broken white lines* in **B**. The *blue*, *red*, and *yellow arrows* in **A, B,** and **C** indicate β-zone PPA margin, Bruch's membrane (BM) opening, and optic disc margin, respectively. The *red*, *blue*, and *yellow* 2-directional arrows in **C** show β-zone PPA width, β-zone PPA with BM (PPA_{+BM}) width, and β-zone PPA without BM (PPA_{-BM}) width, respectively.

PPA_{+BM}, and PPA_{-BM} were measured on the IR images in synchronization with the OCT B-scan images (Fig 1). All OCT B-scan images that were analyzed in the current study were obtained before the VF tests.

Eyes were classified into 3 groups based on the extent of BM opening within the β-zone PPA area on the horizontal scan image: group A (only PPA_{+BM}), group B (both PPA_{+BM} and PPA_{-BM}), and group C (only PPA_{-BM}) (Fig 2). Two examiners (H.Y. and T.A.) evaluated the classification of each type of PPA on the B-scan images. Evaluators were masked to all other patient and ocular data, and eyes were excluded from analyses if a consensus could not be reached.

Calculation of Optic Disc Size Based on Bruch's Membrane Openings

The OCT B-scan images were analyzed, along both horizontal and vertical lines, to measure optic disc size. The distances between the 2 BM openings on the horizontal and vertical B-scan images were measured as the minor and major axis, respectively. The optic disc size was then calculated on the basis of the BM openings, on the assumption that the optic disc is an ellipse.

Statistical Analyses

To evaluate the interobserver reproducibility of β-zone PPA, PPA_{-BM}, and PPA_{+BM} width measurements, evaluations were performed by 2 examiners blinded to any information other than the OCT B-scan images in 50 randomly selected eyes. Intraclass correlation coefficients (ICCs) were then calculated with their confidence intervals. Differences in continuous variables among the 3 groups were compared using a 1-way analysis of variance test with Tukey's post hoc test, and categoric variables were compared using Fisher exact test. Pearson correlation coefficients were calculated to evaluate the relationship between mean deviation (MD) slope and each PPA parameter (β-zone PPA, PPA_{-BM}, and PPA_{+BM} widths on horizontal scans and mean widths of β-zone PPA, PPA_{-BM}, and PPA_{+BM}). The total deviation (TD) slope was obtained by averaging the TD values that occurred in the superior and inferior hemifields during the follow-up period. In eyes with superior or inferior hemifield VF defects, the relationship between each hemifield TD slope and each PPA measurement (β-zone PPA, PPA_{-BM} and PPA_{+BM} widths on upper and lower scans) was analyzed using Pearson correlation coefficients. A general linear model was used to evaluate the influence of several factors (age, sex, axial length, central corneal thickness, optic disc size based on BM opening, history of cataract surgery, history of glaucoma surgery, history of disc hemorrhage, baseline IOP, mean IOP, IOP fluctuation, baseline MD, β-zone PPA width, PPA_{-BM} and PPA_{+BM} width on horizontal scan, mean β-zone PPA width, and mean PPA_{-BM} and PPA_{+BM} width) on glaucoma VF progression with the univariate. Stepwise multiple regression analyses were performed to evaluate the effects of all factors applied in the univariate analysis on VF progression. Subjects with a history of cataract or glaucoma surgery at the beginning of this study were treated in the same way as those without this history. On the other hand, in patients who underwent such surgery during follow-up, only the data collected before surgery were analyzed. Statistical analyses were performed using the Statistical Package for Social Sciences (SPSS version 19.0; International Business Machines Corp, Armonk, NY). P values < 0.05 were considered statistically significant.

Results

Initially, 155 subjects met the inclusion criteria for this study; 16 were excluded because a consensus could not be reached by the 2 examiners classifying the PPA on the horizontal scan images; a further 10 were excluded because they had (1) a BCVA <20/40 (n = 1), (2) a history of eye trauma (n = 1), or (3) upper or lower B-scan OCT images of unacceptable quality (n = 8). As a result, 129 eyes of 129 participants were analyzed.

Comparison of Demographic and Clinical Characteristics of the 3 Groups

Of the 129 included eyes, 39 eyes were classified into group A, 75 eyes were classified into group B, and 15 eyes were classified into group C (Table 1). There were significant differences in age, spherical equivalent, axial length, and MD slope among the 3 groups. The mean age of group A was greater than that of group C ($P = 0.007$). Group A cases were less myopic compared with those of groups B and C (spherical equivalent: both $P < 0.001$, axial length: $P = 0.004$ and $P = 0.007$, respectively). Visual field progression in group A was statistically faster than in group C ($P = 0.004$). Supplemental Figure 1 (available at www.aaojournal.org) shows the relationship between age and MD slope in groups A and C. The MD slope tended to be faster with age in both groups, although there was no significant correlation.

The mean number of highly myopic eyes (with an axial length >26 mm) was 56 of 129 eyes (43%): 8 of 39 eyes (21%) in group A,

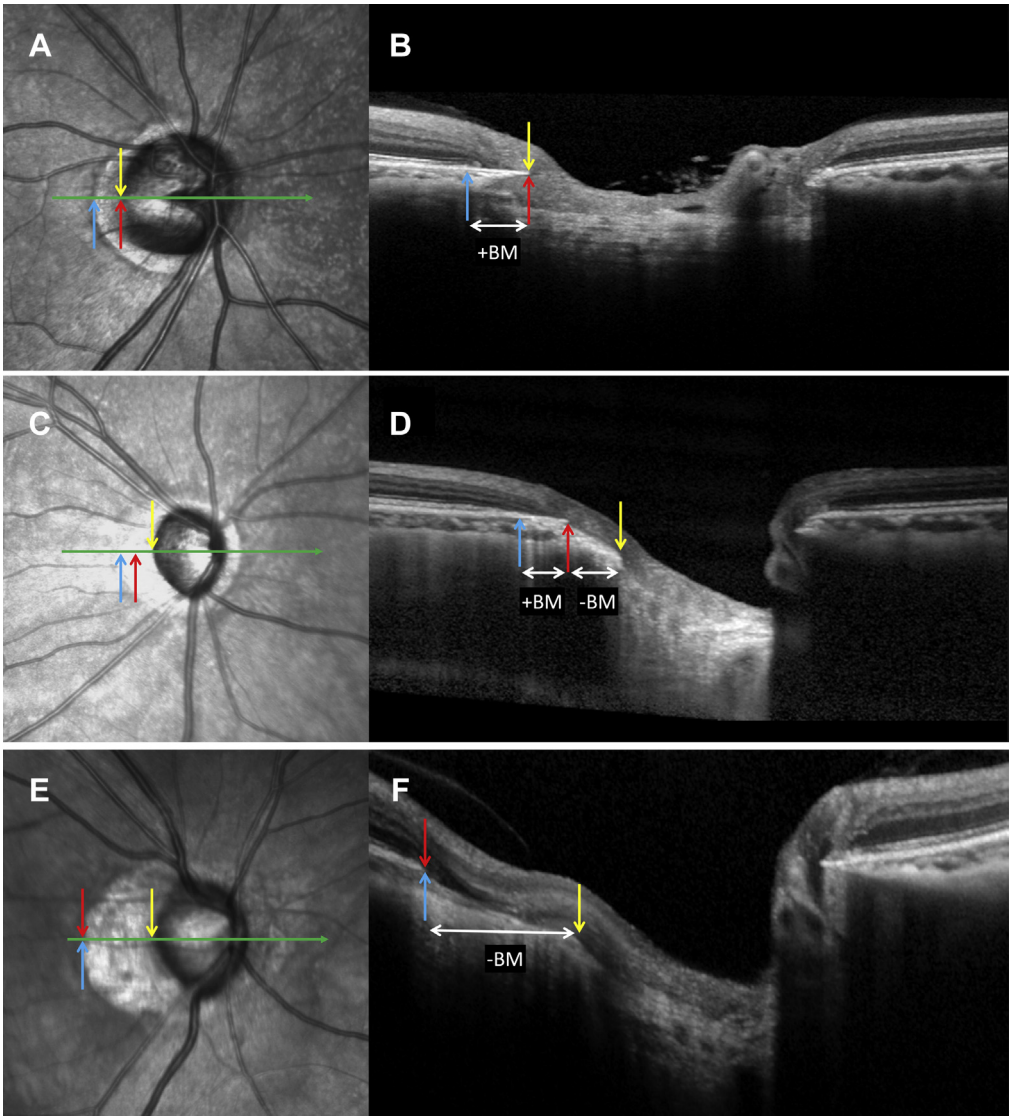

Figure 2. Classification of peripapillary atrophy (PPA) based on the location of Bruch's membrane (BM) opening. **Left**: The infrared (IR) fundus images of the optic disc. **Right**: The spectral-domain optical coherence tomography (SD OCT) images on horizontal cross-sectional scans at the *green arrowed lines* in the **left column**. The *blue*, *red*, and *yellow arrows* indicate β-zone PPA margin, BM opening, and disc margin, respectively. **A, B,** Example of group A. The BM opening is present on the disc margin, and β-zone PPA fully contains BM. **C, D,** Example of group B. The BM opening exists between the disc margin and the β-zone PPA margin. **E, F,** Example of group C. The BM opening exists on the β-zone PPA margin. β-zone PPA does not contain BM.

38 of 75 eyes (51%) in group B, and 10 of 15 eyes (67%) in group C. To examine if the relationship between $PPA_{+BM/-BM}$ and subsequent VF progression could be applied to highly myopic subjects, we subanalyzed using only highly myopic eyes (Supplemental Table S1, available at www.aaojournal.org). There was no significant difference in age, spherical equivalent, and axial length among the 3 highly myopic groups ($P = 0.471$, $P = 0.456$, and $P = 0.302$, respectively), whereas VF progression was faster in group A than in group B or C ($P = 0.033$).

Measurement of β-Zone Peripapillary Atrophy

The ICCs for the measurements of β-zone PPA width, PPA_{+BM} width, and PPA_{-BM} width on 3 scans were excellent (ICC >0.90) (Supplemental Table S2, www.aaojournal.org). In group A, 24 of 39 eyes (62%) exhibited only PPA_{+BM} on both upper and lower line scans, whereas the others contained PPA_{-BM} components on the upper or lower line scan. In group B, 64 of 75 eyes (85%) showed both PPA_{+BM} and PPA_{-BM} components on both upper and lower line scans; however, the remaining eyes exhibited only the PPA_{+BM} or PPA_{-BM} component on the upper or lower line scan. In group C, none of the 15 eyes showed only PPA_{-BM} on both the upper and lower line scans.

Correlation between Axial Length and β-Zone Peripapillary Atrophy

The axial length was significantly correlated with both the β-zone PPA ($r = 0.562$, $P < 0.001$) and the PPA_{-BM} ($r = 0.546$, $P < 0.001$) on the horizontal scans, and it was correlated with

Table 1. Characteristics of Study Groups

Variable	Group A: PPA_{+BM} Only (n = 39)	Group B: PPA_{+BM} and PPM_{-BM} (n = 75)	Group C: PPA_{-BM} Only (n = 15)	*P* Value	Post Hoc Test
Age (yrs)	64.4±12.2 (35–84)	60.0±12.1 (32–87)	53.3±9.8 (30–65)	**0.009***	A > C
Sex (men/women)	21/18	38/37	8/7	0.967†	
Spherical equivalent (D)	−3.25±3.89 (−14.88 to 1.37)	−5.97±3.83 (−15.38 to 1.50)	−8.27±3.28 (−14.38 to −2.88)	**<0.001***	A > B, C
Axial length (mm)	25.00±1.96 (22.01–30.17)	26.13±1.72 (22.24–30.24)	26.65±1.44 (24.13–29.86)	**0.001***	A < B, C
Follow-up duration (yrs)	5.4±1.3 (2–7)	5.3±1.5 (2–9)	5.4±1.6 (2–8)	0.849*	
Central corneal thickness (μm)	516.9±26.4 (464–576)	530.4±32.4 (453–640)	528.5±31.0 (467–574)	0.081*	
Optic disc size on clinical examination (mm^2)	2.19±0.42 (1.40–3.35)	2.14±0.56 (0.96–3.99)	2.36±0.89 (1.27–5.09)	0.400*	
Optic disc size based on BM opening (mm^2)	2.17±0.51 (1.40–3.58)	2.35±0.52 (1.26–3.65)	2.44±0.56 (1.71–4.06)	0.134*	
Baseline IOP (mmHg)	15.3±2.1 (11–20)	15.6±3.0 (10–23)	14.9±2.8 (10–21)	0.569*	
Mean IOP (mmHg)	14.8±1.5 (11.6–19.0)	14.8±1.8 (10.1–19.3)	14.3±2.2 (9.8–19.2)	0.525*	
Last IOP (mmHg)	14.2±1.8 (11–19)	14.0±2.2 (9–20)	13.9±2.3 (12–19)	0.868*	
IOP fluctuation (mmHg)	1.8±0.5 (1.0–3.3)	1.9±0.5 (0.9–3.3)	1.8±0.6 (1.0–2.7)	0.713*	
With/without history of cataract surgery (n)	5/34	4/71	0/15	0.252†	
With/without history of glaucoma surgery (n)	2/37	1/74	0/15	0.497†	
With/without disc hemorrhage (n)	9/30	17/58	1/14	0.382†	
Baseline MD (dB)	−6.7±5.0 (−17.1 to −0.1)	−7.7±6.1 (−22.4 to 0.6)	−9.7±761 (−23.6 to 0.3)	0.234*	
Last MD (dB)	−8.5±5.4 (−23.6 to −0.4)	−8.9±6.2 (−23.8 to 0.7)	−10.1±8.0 (−22.8 to −0.9)	0.762*	
MD slope (dB/y)	−0.46±0.45 (−1.63 to 0.44)	−0.30±0.36 (−1.68 to 0.38)	−0.07±0.39 (−0.97 to 0.56)	**0.005***	A < C
Total No. of SAP (n)	8.5±5.1 (5–23)	10.1±5.5 (5–24)	8.3±3.9 (5–18)	0.213*	
Baseline glaucoma medication (n)	1.1±0.9 (0–3)	1.0±1.0 (0–3)	0.9±1.0 (0–3)	0.763*	
Last glaucoma medication (n)	2.3±1.0 (1–4)	2.0±1.2 (0–4)	1.9±1.8 (0–5)	0.350*	
β-zone PPA width on horizontal scan (μm)	356.2±211.5 (122–1037)	692.0±343.7 (177–1464)	446.7±267.8 (107–893)	**<0.001***	A, C < B
PPA_{-BM} width on horizontal scan (μm)	0	365.3±261.1 (28–1119)	446.7±267.8 (107–893)	n/a	
PPA_{+BM} width on horizontal scan (μm)	356.2±211.5 (122–1037)	325.7±189.7 (29–938)	0	n/a	
Mean β-zone PPA width (μm)	327.1±188.2 (114–919)	621.4±304.5 (184–1436)	483.3±220.4 (165–863)	**<0.001***	A < B
Mean PPA_{-BM} width (μm)	21.7±45.6 (0–219)	330.4±232.1 (9–976)	393.3±228.1 (73–768)	**<0.001***	A < B, C
Mean PPA_{+BM} width (μm)	304.5±174.7 (114–919)	291.2±143.3 (49–817)	90.4±52.3 (21–202)	**<0.001***	A, B > C

BM = Bruch's membrane; D = diopters; dB = decibels; IOP = intraocular pressure; MD = mean deviation; n/a = not applicable; PPA = peripapillary atrophy; PPA_{+BM} = β-zone PPA with Bruch's membrane; PPA_{-BM} = β-zone PPA without Bruch's membrane; SAP = standard automated perimetry.
Values comprise mean ± standard deviation (range).
*Comparison was performed using 1-way analysis of variance with post hoc Tukey's test to compare the differences among the 3 groups.
†Comparison was performed using Fisher exact test. Statistically significant values are in bold.

PPA_{+BM} on the horizontal scan, albeit without significance ($r = 0.171$, $P = 0.053$). Furthermore, axial length was significantly correlated with the mean β-zone PPA, PPA_{+BM}, and PPA_{-BM} of the 3 scans ($r = 0.596$, $P < 0.001$; $r = 0.260$, $P = 0.003$; and $r = 0.552$, $P < 0.001$, respectively).

Risk Factors Associated with Visual Field Progression

We compared VF progression with β-zone PPA, PPA_{+BM}, and PPA_{-BM} widths for all the included eyes. Smaller PPA_{-BM} and larger PPA_{+BM} width on horizontal scans and larger mean PPA_{+BM} width were significantly associated with a faster MD slope in the univariate analysis ($P = 0.019$, $P < 0.001$, and $P < 0.001$, respectively) (Table 2). In the multivariate analysis, there was a weak correlation between the MD slope and the PPA_{+BM} and PPA_{-BM} widths on the horizontal scans ($P < 0.001$ and $P = 0.034$, respectively) and the mean value of the 3 scans ($P < 0.001$ and $P = 0.030$, respectively). There was no correlation between MD slope and horizontal or mean β-zone PPA width of the 3 scans (Table 2, Fig 3).

In a subanalysis of the highly myopic group, the multivariate analysis demonstrated that a disc hemorrhage history, PPA_{+BM} width on horizontal scans, and a mean PPA_{+BM} width of the 3 scans were significantly associated with faster VF progression ($P = 0.009$ or $P = 0.040$, $P < 0.001$ and $P < 0.001$, respectively) (Supplemental Table S3, www.aaojournal.org).

Analysis of Subjects with Unilateral Hemifield Visual Field Defect

In the 129 subjects, there were 31 eyes with superior hemifield VF defect and 26 eyes with inferior hemifield VF defect. The demographic and clinical characteristics of these eyes are presented in Table 3. The eyes with inferior hemifield VF defects were significantly more myopic than those with superior hemifield VF defects (spherical equivalent [$P = 0.015$]; axial length [$P = 0.024$]); they were also less progressive, although this did not constitute a significant difference ($P = 0.064$). There were no differences in any of the other factors between the 2 groups.

The association between the VF progression of unilateral hemifield VF defects and the difference in PPA microstructure in the corresponding location was then examined. In the eyes with superior VF defect only, a longer PPA_{+BM} in the lower scan showed a significant correlation with faster subsequent VF progression ($P = 0.037$); however, there was no significant correlation between β-zone PPA and PPA_{-BM} width (Table 4). In the eyes with inferior VF defect only, the faster VF progression was positively correlated with PPA_{+BM} width of the upper scan ($P = 0.020$) and negatively correlated with PPA_{-BM} width of lower scan ($P = 0.032$). The remaining PPA microstructural parameters did not correlate with VF progression.

Discussion

In the current study, we subclassified POAG eyes according to the presence or absence of BM in β-zone PPA at the temporal side of the optic disc and examined the subsequent VF progression. A significant difference among eyes with different types of β-zone PPA microstructure was observed.

Eyes exhibiting only PPA with intact BM (group A) showed significantly faster VF progression than the eyes exhibiting PPA without BM (groups B and C). This finding is consistent with the results from the study by Kim et al,[13] which showed differences in the rate of retinal nerve fiber layer thinning according to PPA type, although subjects with more than 6 diopters of myopia were excluded in

Table 2. Risk Factors Associated with Glaucomatous Visual Field Progression

Variable	Univariate Analysis		Multivariate Analysis 1		Multivariate Analysis 2	
	β	*P Value*	*β*	*P Value*	*B*	*P Value*
Age (yrs)	−0.113	0.202		0.455		0.209
Sex (men)	−0.046	0.608		0.744		0.818
Axial length (mm)	0.039	0.662		0.957		0.523
Central corneal thickness (μm)	−0.005	0.956		0.744		0.681
Optic disc size based on BM opening (mm^2)	−0.032	0.715		0.795		0.991
History of cataract surgery	0.019	0.833		0.357		0.505
History of glaucoma surgery	0.054	0.542		0.228		0.277
History of disc hemorrhage	−0.139	0.115		0.133		0.221
Baseline IOP (mmHg)	0.024	0.788		0.522		0.481
Mean IOP (mmHg)	−0.023	0.796		0.879		0.910
IOP fluctuation (mmHg)	0.011	0.899		0.622		0.560
Baseline MD (dB)	−0.055	0.534		0.568		0.646
β-zone PPA width on horizontal scan (μm)	−0.064	0.470		0.909		
PPA_{-BM} width on horizontal scan (μm)	**0.206**	**0.019**	**0.175**	**0.034**		
PPA_{+BM} width on horizontal scan (μm)	**−0.368**	**<0.001**	**−0.352**	**<0.001**		
Mean β-zone PPA width (μm)	−0.072	0.418				0.094
Mean PPA_{-BM} width (μm)	0.167	0.058			**0.177**	**0.030**
Mean PPA_{+BM} width (μm)	**−0.381**	**<0.001**			**−0.386**	**<0.001**

BM = Bruch's membrane; dB = decibels; IOP = intraocular pressure; MD = mean deviation; PPA = peripapillary atrophy; PPA_{+BM} = β-zone PPA with Bruch's membrane; PPA_{-BM} = β-zone PPA without Bruch's membrane.
Statistically significant values are in bold.

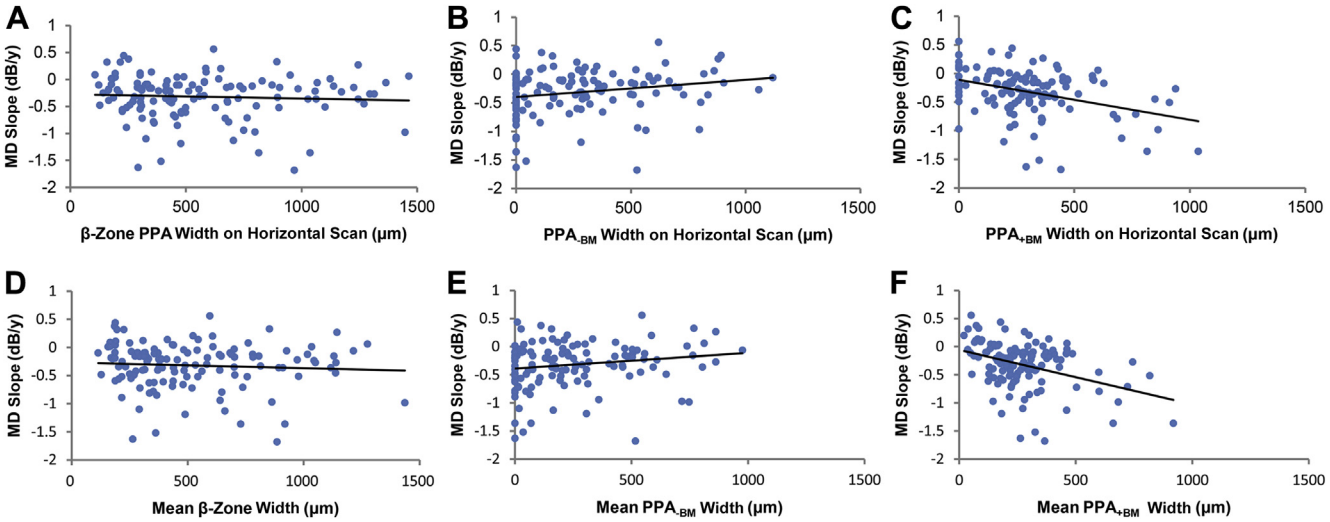

Figure 3. Scatterplots showing the relationship between the mean deviation (MD) slope and the microstructure widths of peripapillary atrophy (PPA) in all included eyes. **A**, Horizontal β-zone PPA width and MD slope are not significantly correlated ($P = 0.470$). **B,** Horizontal PPA_{-BM} width and MD slope show a slightly significant positive correlation ($P = 0.019$). **C**, Horizontal PPA_{+BM} width and MD slope are significantly negatively correlated ($P < 0.001$). **D**, Mean width of β-zone PPA and MD slope are not significantly correlated ($P = 0.418$). **E**, Mean width of PPA_{-BM} and MD slope show marginal correlation without significance ($P = 0.058$). **F**, Mean width of PPA_{+BM} is significantly negatively correlated with MD slope ($P < 0.001$). dB = decibels; PPA_{+BM} = β-zone PPA with Bruch's membrane; PPA_{-BM} = β-zone PPA without Bruch's membrane.

their study. We also found the same relationship between VF progression and microstructure of β-zone PPA in the subanalysis including only highly myopic subjects (Supplementary Table S1, www.aaojournal.org). These results suggest that the influence of PPA type on glaucoma progression is applicable not only to nonhighly myopic glaucomatous eyes but also to glaucomatous eyes with high myopia.

Myopia is a well-known risk factor for the development of glaucoma.[19–23] However, there is still controversy regarding myopia as a glaucoma progression risk.[23–25] In the current study, myopia did not significantly influence VF progression according to univariate and multivariate analyses (Table 2). It was not possible to determine whether myopia is a risk for glaucoma progression in our study because of the small sample size. Different types of eyes

Table 3. Characteristics of Eyes with Unilateral Hemifield Visual Defect

Variable	Superior Visual Field Defect (n=31)	Inferior Visual Field Defect (n=26)	P Value*
Age (yrs)	60.3±12.9 (36–84)	59.6±11.4 (30–83)	0.820
Spherical equivalent (D)	−3.76±3.74 (−11.50 to 1.25)	−6.20±3.55 (−15.13 to 0.25)	**0.015**
Axial length (mm)	25.24±1.79 (22.01–29.66)	26.21±1.29 (23.77–28.33)	**0.024**
Central corneal thickness (μm)	519.5±29.0 (453–585)	528.2±27.5 (464–574)	0.253
Optic disc size based on clinical examination (mm^2)	2.19±0.50 (1.46–3.14)	2.36±0.57 (0.96–3.58)	0.236
Optic disc size based on BM opening (mm^2)	2.24±0.46 (1.40–3.10)	2.43±0.46 (1.34–3.57)	0.118
Baseline IOP (mmHg)	14.9±2.9 (10–22)	15.6±2.5 (11–23)	0.301
Mean IOP (mmHg)	14.9±1.6 (11.2–19.0)	15.0±2.0 (11.8–19.3)	0.977
Last IOP (mmHg)	14.1±2.0 (9–19)	14.7±2.6 (11–20)	0.331
IOP fluctuation (mmHg)	1.8±0.5 (0.9–3.0)	1.9±0.6 (0.9–3.3)	0.813
Baseline MD (dB)	−4.9±4.3 (−14.6 to −0.1)	−4.9±3.4 (−13.6 to 0.6)	0.961
Baseline TD (dB)			
Superior hemiretinas	−8.1±7.7 (−26.8 to −0.6)	−1.3±1.6 (−4.0 to 0.9)	n/a
Inferior hemiretinas	−1.6±1.7 (−3.2 to 0.7)	−6.8±5.1 (−18.7 to −0.1)	n/a
MD slope (dB/y)	−0.26±0.34 (−1.10 to 0.44)	−0.10±0.34 (−0.85 to 0.56)	0.064
TD slope (dB/y)			
Superior hemiretinas	−0.40±0.53 (−1.93 to 0.32)	0.02±0.29 (−1.04 to 0.67)	n/a
Inferior hemiretinas	−0.09±0.26 (−0.65 to 0.73)	−0.19±0.43 (−1.32 to 0.71)	n/a

BM = Bruch's membrane; D = diopters; dB = decibels; IOP = intraocular pressure; MD = mean deviation; n/a = not applicable; TD = total deviation. Values comprise mean ± standard deviation (range).
*Comparison was performed using an unpaired *t* test. Statistically significant values are in bold.

Table 4. Coefficients of Correlation between Various Peripapillary Atrophy Widths and Hemifield Visual Defects in Eyes with Hemifield Total Deviation Slopes on the Side with the Visual Field Defects

	Superior Visual Field Defect (n=31)		Inferior Visual Field Defect (n=26)	
	r	*P Value**	*r*	*P Value**
Upper scan				
β-zone PPA width	−0.100	0.592	−0.050	0.809
PPA_{-BM} width	0.020	0.915	0.309	0.125
PPA_{+BM} width	−0.214	0.247	**−0.453**	**0.020**
Lower scan				
β-zone PPA width	−0.138	0.460	0.214	0.294
PPA_{-BM} width	−0.023	0.901	**0.421**	**0.032**
PPA_{+BM} width	**−0.375**	**0.037**	−0.387	0.051

PPA = peripapillary atrophy; PPA_{+BM} = β-zone PPA with Bruch's membrane; PPA_{-BM} = β-zone PPA without Bruch's membrane.
r and *Pearson's correlation coefficient. Statistically significant values are in bold.

exhibit varying speeds of progression, even in glaucomatous eyes with myopia. A number of previous studies have reported an association between the β-zone PPA and the presence of glaucoma[1–3,5–7] or glaucoma progression.[4–8] However, the presence of β-zone PPA is not always useful for the detection of glaucoma because β-zone PPA is common in myopic eyes.[9] The microstructure of β-zone PPA may provide useful information for the evaluation of glaucomatous eyes with high myopia, although further studies with larger myopic samples are required to clarify this issue.

We found that a larger PPA_{+BM} was significantly associated with faster subsequent VF progression. It has been suggested that PPA_{+BM} is an age-related ongoing process.[13,14] Our results suggest that the atrophic change in the choroid not only is a result of glaucoma but also plays an important role in its progression. In contrast, PPA_{-BM} has been proposed to be related to the scleral stretch with myopic change.[12–15,17] In the present study, we found that a larger PPA_{-BM} was significantly associated with slower VF progression, suggesting the possibility that an extension of PPA_{-BM} may have an inhibitory effect on glaucoma progression. The extension of PPA_{-BM} may reduce stress to the lamina cribrosa when axial elongation occurs with increasing myopia.

In the eyes with superior or inferior hemifield VF defects, we report a longer PPA_{+BM} at the corresponding side of VF defects correlated with a poorer hemifield TD slope. This could mean that the atrophic change at the peripapillary area influences the corresponding VF progression. Teng et al[26] reported that the location of the largest β-zone PPA correlated with the region exhibiting the most rapid subsequent VF progression in patients with treated open-angle glaucoma. In the current study, we did not find a significant correlation between TD slope and β-zone PPA width; however, there was a significant correlation with PPA_{+BM}. This discrepancy most likely relates to the variations in subject populations between studies. Teng et al[26] included only patients with less than 6 diopters; however, numerous highly myopic eyes were included in the current study. Our results indicate that PPA_{+BM} has a greater influence on VF progression than β-zone PPA, especially in highly myopic patients. In contrast, we found that a longer PPA_{+BM} at the noncorresponding side also marginally correlated with faster VF progression in the eyes with inferior hemifield VF defects. Further investigation would be needed to clarify the relationship between PPA location and VF progression, and the mechanism behind this.

In eyes with superior hemifield VF defects, longer PPA_{-BM} was not correlated with slower VF progression; however, PPA_{-BM} was significantly correlated at the noncorresponding side, and a trend was found at the corresponding side in eyes with inferior hemifield VF defects (Table 4). This suggests that these 2 types of glaucoma present different characteristics. Kawano et al[27] reported that, in the eyes with normal-tension glaucoma, the inferior half area of β-zone PPA significantly correlated with VF defect and myopia; however, the superior half area of β-zone PPA correlated only with myopia. This supports our finding that PPA_{-BM} may act protectively for glaucoma progression and attention on PPA_{-BM} is warranted, especially in eyes with inferior VF defects or myopia.

We classified our subjects into 3 groups based on the microstructure of PPA on horizontal OCT images, as previously reported.[13,14] However, the current study revealed that the classification derived from PPA microstructure was not always consistent among the 3 OCT image scans (agreement rate in this study: 68.2% [88/129 eyes]), as described earlier. Our OCT image scans were performed on the horizontal axis of the acquired image frame of the imaging device, as opposed to the fovea−BM opening center axis. Therefore, the classification into 3 groups in this study may not be conclusive because of the upper and lower scans misrepresenting the locations at the same angle from a fovea-BM opening center axis. Peripapillary atrophy evaluations based on a fovea-BM opening center axis would be more favorable in future investigations.

The eyes in group C showed slower VF progression than those in group A; however, there was no statistical difference in MD value between these groups. We cannot adequately explain the reason for this discrepancy. The eyes in group C were predominately highly myopic. High myopia is known to be a risk factor for glaucoma development; however, the relationship between high myopia and glaucoma progression is still controversial.[23–25] It could be presumed that VF progression occurred at an earlier stage in group C, but did not continue to worsen. Further investigation is necessary to clarify the timing and pattern associated with the worsening of VF in eyes with PPA_{-BM}.

Study Limitations

First, this was a retrospective cohort study. Therefore, selection bias may have occurred with regard to baseline variables because this study included untreated patients or patients receiving medical and surgical treatment. For

example, the IOP-related variables, including baseline IOP, mean IOP, and IOP fluctuation are known to be associated with glaucoma progression;[8,28–34] however, this was not observed in the current study. Furthermore, although thin central corneal thickness and large optic discs are also reported to be risk factors for glaucoma progression,[28,29] these relationships were not found to exist among our subjects.[28,29] A prospective cohort study with a large sample size is needed to clarify the relationship between the factors involved in glaucoma progression. Second, the β-zone PPA, PPA_{+BM}, and PPA_{-BM} widths measured in this study were not always the actual widths. We measured these widths linearly on the plane images without considering optic globe curvature. Axial elongation often tends to result in posteriorly curved surface of PPA; therefore, the shortly estimated potentiality, especially in axially elongated eyes, needs to be considered. Third, we analyzed only temporal β-zone PPA in radial B-scan images, although β-zone PPA was present in areas other than the temporal region. Analyzing the entire β-zone PPA may provide further information; however, we only analyzed the temporal area of the optic disc because this area is more likely to be damaged in glaucoma. Moreover, because of vessel shadowing, it can be difficult to measure PPA microstructure widths using OCT B-scan images in the other regions.

In conclusion, VF progression differed depending on β-zone PPA microstructure in POAG; this was true even in highly myopic eyes. The PPA_{+BM} width may be an important risk factor for VF progression in POAG, and PPA_{-BM} may have a protective effect in a subset of eyes with POAG.

Acknowledgments. The authors thank Akiko Hirata for PPA microstructure measurements in the evaluation of ICC.

References

1. Jonas JB, Nguyen XN, Gusek GC, Naumann GO. Parapapillary chorioretinal atrophy in normal and glaucoma eyes. I. Morphometric data. Invest Ophthalmol Vis Sci 1989;30:908–18.
2. Jonas JB. Clinical implications of peripapillary atrophy in glaucoma. Curr Opin Ophthalmol 2005;16:84–8.
3. Jonas JB, Naumann GO. Parapapillary chorioretinal atrophy in normal and glaucoma eyes. II. Correlations. Invest Ophthalmol Vis Sci 1989;30:919–26.
4. Lee EJ, Kim TW, Weinreb RN, et al. Beta-Zone parapapillary atrophy and the rate of retinal nerve fiber layer thinning in glaucoma. Invest Ophthalmol Vis Sci 2011;52:4422–7.
5. Teng CC, De Moraes CG, Prata TS, et al. Beta-Zone parapapillary atrophy and the velocity of glaucoma progression. Ophthalmology 2010;117:909–15.
6. Daugeliene L, Yamamoto T, Kitazawa Y. Risk factors for visual field damage progression in normal-tension glaucoma eyes. Graefes Arch Clin Exp Ophthalmol 1999;237:105–8.
7. Uchida H, Ugurlu S, Caprioli J. Increasing peripapillary atrophy is associated with progressive glaucoma. Ophthalmology 1998;105:1541–5.
8. Araie M, Sekine M, Suzuki Y, Koseki N. Factors contributing to the progression of visual field damage in eyes with normal-tension glaucoma. Ophthalmology 1994;101:1440–4.
9. Ramrattan RS, Wolfs RC, Jonas JB, et al. Determinants of optic disc characteristics in a general population: the Rotterdam Study. Ophthalmology 1999;106:1588–96.
10. Jonas JB, Gusek GC, Naumann GO. Optic disk morphometry in high myopia. Graefes Arch Clin Exp Ophthalmol 1988;226:587–90.
11. Akagi T, Hangai M, Kimura Y, et al. Peripapillary scleral deformation and retinal nerve fiber damage in high myopia assessed with swept-source optical coherence tomography. Am J Ophthalmol 2013;155:927–36.
12. Jonas JB, Jonas SB, Jonas RA, et al. Parapapillary atrophy: histological gamma zone and delta zone. PLoS One 2012;7:e47237.
13. Kim YW, Lee EJ, Kim TW, et al. Microstructure of beta-zone parapapillary atrophy and rate of retinal nerve fiber layer thinning in primary open-angle glaucoma. Ophthalmology 2014;121:1341–9.
14. Kim M, Kim TW, Weinreb RN, Lee EJ. Differentiation of parapapillary atrophy using spectral-domain optical coherence tomography. Ophthalmology 2013;120:1790–7.
15. Dai Y, Jonas JB, Huang H, et al. Microstructure of parapapillary atrophy: beta zone and gamma zone. Invest Ophthalmol Vis Sci 2013;54:2013–8.
16. Reis AS, Sharpe GP, Yang H, et al. Optic disc margin anatomy in patients with glaucoma and normal controls with spectral-domain optical coherence tomography. Ophthalmology 2012;119:738–47.
17. Hayashi K, Tomidokoro A, Lee KY, et al. Spectral-domain optical coherence tomography of beta-zone peripapillary atrophy: influence of myopia and glaucoma. Invest Ophthalmol Vis Sci 2012;53:1499–505.
18. Anderson D, Patella V. Interpretation of a single field. In: Anderson D, Patella V, eds. Automated Static Perimetry. 2nd ed. St. Louis, MO: Mosby; 1999:121–90.
19. Xu L, Wang Y, Wang S, et al. High myopia and glaucoma susceptibility the Beijing Eye Study. Ophthalmology 2007;114:216–20.
20. Mitchell P, Hourihan F, Sandbach J, Wang JJ. The relationship between glaucoma and myopia: the Blue Mountains Eye Study. Ophthalmology 1999;106:2010–5.
21. Grodum K, Heijl A, Bengtsson B. Refractive error and glaucoma. Acta Ophthalmol Scand 2001;79:560–6.
22. Wong TY, Klein BE, Klein R, et al. Refractive errors, intraocular pressure, and glaucoma in a white population. Ophthalmology 2003;110:211–7.
23. Chihara E, Liu X, Dong J, et al. Severe myopia as a risk factor for progressive visual field loss in primary open-angle glaucoma. Ophthalmologica 1997;211:66–71.
24. Lee YA, Shih YF, Lin LL, et al. Association between high myopia and progression of visual field loss in primary open-angle glaucoma. J Formos Med Assoc 2008;107:952–7.
25. Sohn SW, Song JS, Kee C. Influence of the extent of myopia on the progression of normal-tension glaucoma. Am J Ophthalmol 2010;149:831–8.
26. Teng CC, De Moraes CG, Prata TS, et al. The region of largest beta-zone parapapillary atrophy area predicts the location of most rapid visual field progression. Ophthalmology 2011;118:2409–13.
27. Kawano J, Tomidokoro A, Mayama C, et al. Correlation between hemifield visual field damage and corresponding parapapillary atrophy in normal-tension glaucoma. Am J Ophthalmol 2006;142:40–5.

28. Hayamizu F, Yamazaki Y, Nakagami T, Mizuki K. Optic disc size and progression of visual field damage in patients with normal-tension glaucoma. Clin Ophthalmol 2013;7:807–13.
29. Leske MC, Heijl A, Hyman L, et al. Predictors of long-term progression in the early manifest glaucoma trial. Ophthalmology 2007;114:1965–72.
30. Nouri-Mahdavi K, Hoffman D, Coleman AL, et al. Predictive factors for glaucomatous visual field progression in the Advanced Glaucoma Intervention Study. Ophthalmology 2004;111:1627–35.
31. Stewart WC, Kolker AE, Sharpe ED, et al. Factors associated with long-term progression or stability in primary open-angle glaucoma. Am J Ophthalmol 2000;130:274–9.
32. Comparison of glaucomatous progression between untreated patients with normal-tension glaucoma and patients with therapeutically reduced intraocular pressures. Collaborative Normal-Tension Glaucoma Study Group. Am J Ophthalmol 1998;126:487–97.
33. Nakagami T, Yamazaki Y, Hayamizu F. Prognostic factors for progression of visual field damage in patients with normal-tension glaucoma. Jpn J Ophthalmol 2006;50:38–43.
34. Lee KY, Tomidokoro A, Sakata R, et al. Cross-sectional anatomic configurations of peripapillary atrophy evaluated with spectral domain-optical coherence tomography. Invest Ophthalmol Vis Sci 2010;51:666–71.

Footnotes and Financial Disclosures

Originally received: July 18, 2015.
Final revision: October 20, 2015.
Accepted: October 28, 2015.
Available online: December 12, 2015. Manuscript no. 2015-1212.

Department of Ophthalmology and Visual Sciences, Kyoto University Graduate School of Medicine, Kyoto, Japan.

Financial Disclosure(s):
The author(s) have made the following disclosure(s): T.A.: Grants pending – Japan Society for the Promotion of Science.

H.O.I.: Grants pending – Uehara Memorial Foundation, Japan Foundation for Applied Enzymology, Mochida Memorial Foundation for Medical and Pharmaceutical Research.

N.Y.: Consultant – Canon Inc, Nidek Inc; Grants pending – Novartis, Bayer, Santen, Senju; Lecturer – Novartis, Bayer, Santen, Alcon, Senju, Otsuka, Kowa, MSD, Japan Focus, Canon Inc, Nidek Inc; Receives payment for educational presentations – Novartis and Bayer.

Supported by a Grant-in-Aid for Scientific Research (25462713) from the Japan Society for the Promotion of Science and the Innovative Techno-Hub for Integrated Medical Bio-Imaging of the Project for Developing Innovation Systems, from the Ministry of Education, Culture, Sports, Science, and Technology, Japan. The sponsor or funding organization had no role in the design or conduct of this research.

Author Contributions:

Conception and design: Yamada, Akagi

Data Collection: Yamada, Akagi, Nakanishi, Ikeda, Kimura, Suda, Hasegawa, Yoshikawa, Iida

Analysis and interpretation: Yamada, Akagi, Nakanishi, Ikeda

Obtained funding: Akagi, Yoshimura

Overall responsibility: Yamada, Akagi

Abbreviations and Acronyms:
BCVA = best-corrected visual acuity; **BM** = Bruch's membrane; **ICC** = intraclass correlation coefficient; **IOP** = intraocular pressure; **IR** = infrared; **MD** = mean deviation; **OCT** = optical coherence tomography; **POAG** = primary open-angle glaucoma; **PPA** = peripapillary atrophy; $\mathbf{PPA_{+BM}}$ = β-zone PPA with Bruch's membrane; $\mathbf{PPA_{-BM}}$ = β-zone PPA without Bruch's membrane; **SAP** = standard automated perimetry; **SD OCT** = spectral-domain optical coherence tomography; **TD** = total deviation; **VF** = visual field.

Correspondence:
Tadamichi Akagi, MD, PhD, Department of Ophthalmology and Visual Sciences, Kyoto University Graduate School of Medicine, 54 Shougoin Kawahara-cho, Sakyo-ku, Kyoto 606-8507, Japan. E-mail: akagi@kuhp.kyoto-u.ac.jp.